

Functional Micro/Macro Fabrication Combining Multiple Additive Fabrication Technologies: Design and Development of an Improved Micro-Vane Phacoemulsifier used in Cataract Surgery

Jae-Won Choi^{1,2}, Masaki Yamashita³, Jun Sakakibara³,
Yuichi Kaji⁴, Tetsuro Oshika⁴, and Ryan B. Wicker^{1,2}

¹W.M.Keck Center for 3D Innovation, The University of Texas at El Paso, El Paso, TX 79968, USA

²Department of Mechanical Engineering, The University of Texas at El Paso, El Paso, TX 79968, USA

³Department of Engineering Mechanics and Energy, University of Tsukuba, 309-8573 Tsukuba, Japan

⁴Department of Ophthalmology, Institute of Clinical Medicine, University of Tsukuba, 309-8573 Tsukuba, Japan

Abstract

Microstereolithography (μ SL) technology can fabricate complex, three-dimensional (3D) microstructures, although μ SL has difficulty producing macrostructures with micro-scale features. There are potentially many applications, where 3D micro-features can benefit the overall function of the macrostructure. One such application has been recently identified in cataract surgery where a medical device, called a coaxial phacoemulsifier, is inserted into the eye through a relatively small incision and used to break the lens apart while removing the lens pieces and associated fluid from the eye through a small tube. In order to maintain the eye at a constant pressure, the phacoemulsifier also includes an irrigation solution that is injected into the eye during the procedure. It has been reported, however, that the impinging flow from the irrigation solution on the corneal endothelial cells in the inner eye damages these cells during the procedure. As a result, we are exploring methods for reducing flow velocities during this procedure, and have designed a complex, 3D micro-vane within a sleeve that introduces swirl into the irrigation solution, and thus, produces a flow with rapidly dissipating flow velocities. However, the fabrication of the sleeve could not be accomplished using μ SL alone, and thus, a two-part design was accomplished where a sleeve with the micro-vane was fabricated with μ SL and a threaded fitting used to attach the sleeve to the phacoemulsifier was fabricated using an Objet Eden 333 rapid prototyping machine. The new combined device was tested in a water container using particle image velocimetry, and the results showed an ejection of the irrigation fluid through the micro-vane in three different radial direction. It is believed that this new device will reduce damage to endothelial cells during cataract surgery and significantly improve patient outcomes from this procedure. This unique application demonstrates the utility of combining μ SL with a macro rapid prototyping technology for fabricating a real macro-scale device with functional, 3D micro-scale features that could not be fabricated using conventional methods.

Keywords: Phacoemulsification, Cataract Surgery, Irrigation, Swirl, Microstereolithography

1. Introduction

In cataract surgery, phacoemulsification has been widely used to remove the crystalline, where an ultrasound irrigation and aspiration hand piece emulsifies and removes the internal lens of the eye through incision sites, and an artificial lens is inserted immediately. There are two types of phacoemulsification used in the cataract surgery: bimanual and coaxial. Bimanual phacoemulsification employs two separate stainless pipes for irrigation and aspiration, whereas coaxial phacoemulsification employs a combination of stainless pipe named 'tip' and a dead-ended plastic pipe named 'sleeve', which coaxially surrounds the tip, and where a gap between the tip and sleeve leads irrigation flow. Generally, bimanual phacoemulsification has the advantage of a small incision (1.2 mm – 1.4 mm) in comparison to a relatively large incision (2.8 mm – 3.2 mm) in coaxial phacoemulsification (Gajjar, et al., 2007; Osher and Injev, 2007). Contrarily, coaxial phacoemulsification has advantages of high vacuum level, better temperature control, integrity of the incision, easy handling, less invasive and safer operation, better sealability, and fluidic benefits (Osher and Injev, 2007). Even though the two types of phacoemulsification have advantages and are still in use, it has been reported that the bimanual phacoemulsification has more disadvantages such as limited irrigation by small incisions (Osher and Injev, 2007), chamber instability due to leakage through two incision sites (Lee et al., 2009), greater ingress of bacterial inoculums (Gajjar et al., 2007), and development of mechanical wound trauma due to angular movement of the instruments through the small incision sites (Lee et al., 2009). In the recent advancement, microcoaxial phacoemulsification with an incision of 2.2 mm has been developed such that it can overcome the drawbacks of bimanual and the problem of the large incision of coaxial phacoemulsification, as still having the advantages of coaxial phacoemulsification mentioned above (Gajjar et al., 2007, Lee et al., 2009).

The irrigation solution in phacoemulsification surgery plays an important role in maintaining a constant pressure in the anterior chamber and dissipating heat generated from the ultrasonic tip as well as maintaining an endothelial cell survival by the chemical composition of the solution (Joussen et al., 2000). Despite of the importance of the irrigation solution, several studies have shown that the impinging flow from the irrigation solution on the corneal endothelial cells in the inner eye damages these cells during the procedure (Polack and Sugar, 1976; Binder et al., 1976; Miller et al., 1996; Hayashi et al., 1996; Topaz et al., 2002; O'Brien et al., 2004; Steinert and Schafer, 2006). It is well known that cells including the one in the cornea endothelial layer can be damaged by the tangential component of the hydrodynamic forces, i.e. shear stress, resulting from irrigation (Binder et al., 1976; Born et al., 1992; Thoumine et al., 1995; Kaji et al., 2005).

As a result of the effort to reduce flow velocities during this procedure, it has been suggested to design and fabricate a complex, 3D micro-vane within a sleeve that introduces swirl into the irrigation solution, and thus, produces a flow with rapidly dissipating flow velocities. Although additive manufacturing (AM) systems are capable of producing 3D complex structures, the fabrication of the sleeve with 3D micro-vanes could not be accomplished in one AM system alone because the

sleeve with the micro-vane has both macro- and micro-features. That is, most of commercialized AM systems cannot meet resolution for micro-features, whereas there are several types of lab-based, additive microfabrication systems, which are not suitable for producing macro-structures because of long fabrication time, distortion, weak mechanical strength, and limitation of work volume (Varadan et al., 2001; Choi et al., 2006; Regenfuss et al., 2007; Khalil and Sun et al., 2007; Lee et al., 2008). Therefore, a two-part design is needed, where a sleeve with the micro-vane can be fabricated with a microfabrication system and a threaded fitting used to attach the sleeve to the phacoemulsifier can be fabricated using a commercialized AM system so that they can be assembled after fabrication. Among 3D microfabrication systems for producing a sleeve, it is thought that microstereolithography (μ SL), a technology that evolved from stereolithography (SL), is more compatible than others due to its capability of achieving high resolution ($< 10 \mu\text{m}$), and high-aspect ratio fabrication (Bertsch et al., 1997; Sun et al., 2005; Choi et al., 2009a, 2009b). In addition to the microfabrication, commercial AM systems with high-resolution are recommended for producing a threaded fitting part.

In this work, a two-part design was accomplished, and then a 3D micro-vane within a sleeve and a threaded fitting were fabricated with μ SL and a commercial AM system, respectively. Compared to a commercial AM system, μ SL has more issues associated with microfabrication, for example, requirement of low viscosity material, cure depth control, dimensional accuracy, and distortion after building. For the successful fabrication of a sleeve, the work presented here includes system alignment using a large imager, preparation of a low viscosity photocurable resin using a diluent, cure depth control using a light absorber, curing characteristics test, and multiple exposure for obtaining a micro-vane within a sleeve without bending. Finally the two final parts were integrated with a phacoemulsifier, and particle image velocimetry (PIV) was used to show the reduction of mean velocity distribution in a water container. The followings will describe the two-part design, micro/macrob fabrication, and PIV results in more detail.

2. Experimental apparatus

2.1 Multi-Jet Modeling (MJM)

MJM, also referred to as 3D Printing (3DP), is one of the Additive Manufacturing (AM) processes available, which uses a printer head, ultraviolet light (UV), and a photocurable liquid resin. In this work, an Objet Eden 333 (Objet Geometries Ltd., Billerica, MA) was used for producing a threaded fitting. This system is capable of stacking thin layers with a $16 \mu\text{m}$ thickness by injecting a curing viscous photopolymer through the printer head while simultaneously curing the photopolymer with the UV light. In particular, it utilizes a build and support material separately, and after finishing a build, the support material is removed by using high-pressure water.

2.2 Dynamic mask microstereolithography (μ SL)

For the purpose of producing 3D microstructures, μ SL has been widely used for various engineering applications since its first introduction (Ikuta and Kirowatari, 1993). μ SL technology is based on

stereolithography (SL), and it can be classified into two types: vector-by-vector μ SL, also referred to as scanning μ SL, by scanning a focused laser beam (Ikuta and Kirowatari, 1993; Zissi et al., 1996; Sun and Zhang, 2002; Lee et al., 2007, 2008); and integral μ SL, also referred to as projection μ SL, by projecting an image reflected on a dynamic mask (Bertsch et al., 1997, 2001, 2004; Sun et al., 2005; Choi et al., 2006, 2009a, 2009b; Limaye and Rosen, 2007; Ha et al., 2008; Han et al., 2008).

In this work, Digital Micromirror Device (DMDTM)-based μ SL was used to produce a sleeve with a micro-vane. Fig. 1 shows the μ SL system, which consists of an Omnicure S2000TM as a light source with an output of 200 W, a collimating lens, and an optical fiber (EXFO Co., Canada), a DMDTM with \sim 780,000 micromirrors with the size of 13.68 μ m (DMD Starter Kit, Texas Instruments, USA), a tube lens with a focal length of 120 mm (Achromat doublet lens, MellesGriot Co. USA), an aluminum-coated reflecting mirror, a focusing unit (IM-4, Nikon Co., Japan), an objective lens (CFI Plan Flour 4 \times , Nikon Co., USA), a motor-driven linear Z-stage with a resolution of 1 μ m (ATS100-050, Aerotech, USA), and a stainless resin vat. For the fabrication of microstructures, a desired 3D model is sliced and converted into binary images as cross-sections, which are transferred to the DMDTM board in process. The DMDTM plays a key role in dynamic mask projection μ SL, and each individual micromirror is tilted at $\pm 12^\circ$ according to the binary value, i.e., 0 or 1, so that entire DMDTM forms a certain image. The illuminated light is patterned by being reflected on the DMDTM, delivered to the resin surface through several optics, and finally the focused pattern cures the resin surface with the prescribed thickness. Finally, the Z-stage stacks the cured layers and refreshes new resin surface for the next build, and this continuous builds produce a 3D microstructure. In the developed system, the exposure energy at the resin surface is ~ 26.35 mJ/cm², and the reduction ratio is ~ 0.329 between an image on the DMDTM and resin surface. Although the μ SL system is described briefly here, the interested readers are recommended to read the references (Choi et al., 2006, 2009a, 2009b) for further details of the system.

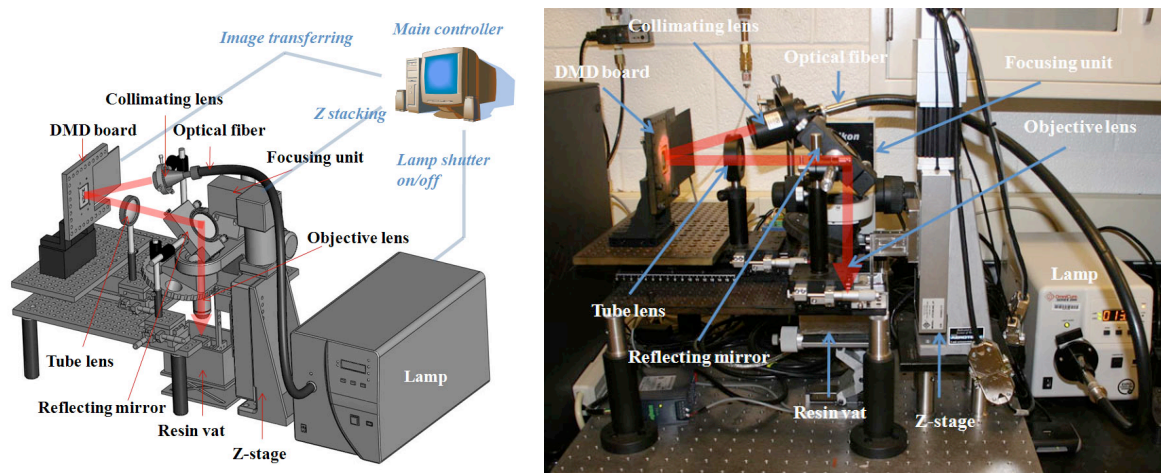


Fig. 1 Developed μ SL system: (a) schematic of the system, (b) photo of the system

3. Materials, Design, and Methods

3.1 Materials

Objet Eden 333 system using Objet FullCure[®] 840 as a build material and FullCure[®] 705 as a support material was utilized to fabricate the threaded fitting. ProtoTherm[™] 12120 was used as a main material in μ SL (DSM Somos[®], New Castle, DE, USA). Propoxylated (2) neopentyl glycol diacrylate (PNGD) (Sartomer Inc., Warrington, PA) was used. To control cure depth, Tinuvin 400 (Ciba Specialty Chemicals, Newport, DE) was added to the ProtoTherm-PNGD mixture.

3.2 Design of sleeve

To replace the original sleeve in a phacoemulsifier with a micro-vane within a sleeve, a two-part design for a threaded fitting fabricated in MJM and the sleeve with the micro-vane fabricated in μ SL was accomplished. The threaded fitting as shown in Fig. 2 consists of a thread, inner channel, and space for the sleeve to be equipped. The sleeve design has a micro-vane as shown in Fig. 3, and the dimensions referred an existing sleeve and tip. The micro-vane as shown in Fig. 3 was generated by sweeping a rectangular section with the size of 0.219 mm \times 0.110 mm along with a spiral curve. The spiral curve consists of two curves, which have a diameter of 1.54 mm and different pitch and revolution as shown in Fig. 3 (b). The upper curve has 1 mm height and 2 mm pitch, and the lower curve has 2 mm height and 10 mm pitch, so that the combined curve has steep and gentle slopes from the bottom to top, which introduces smooth swirl. Fig. 4 shows the 3D model of the assembled sleeve with the threaded fitting.

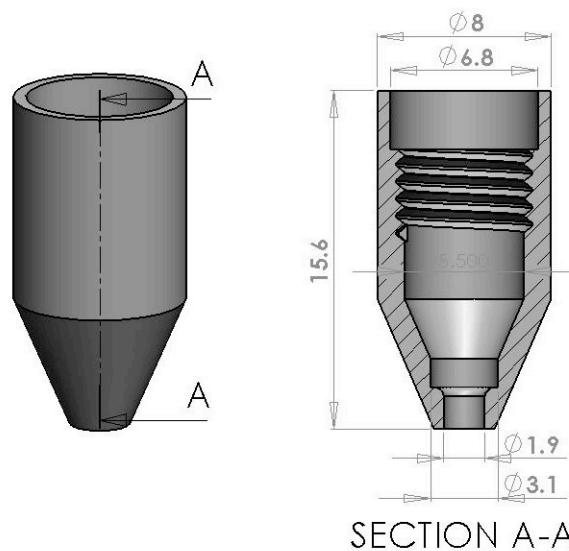


Fig. 2 3D model of the threaded fitting (unit: metric)

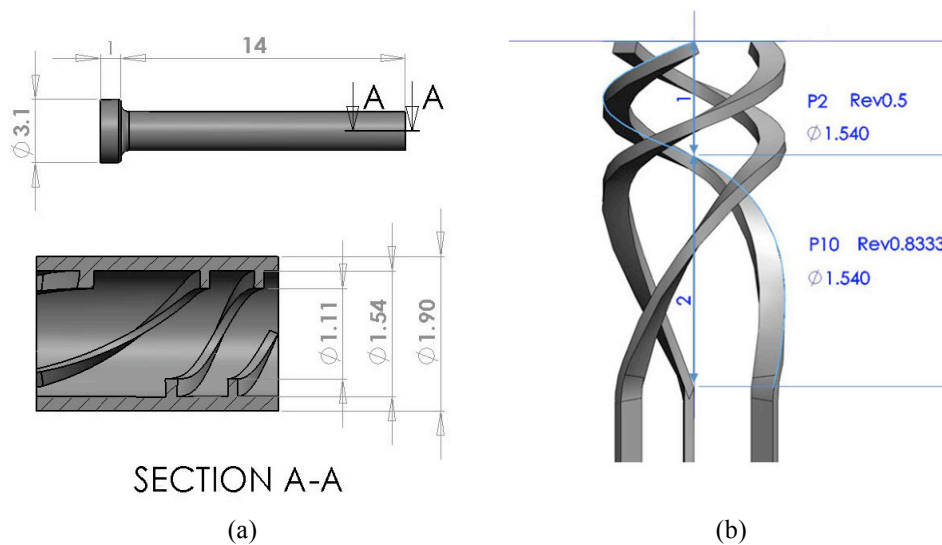


Fig. 3 3D model of the sleeve with micro-vane: (a) hollow tube and section, (b) micro-vane (unit: metric)

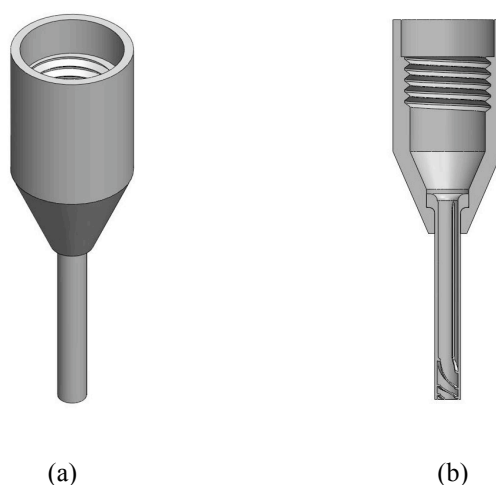


Fig. 4 3D model of the assembled sleeve: (a) 3D model, (b) section

3.3 Methods

3.3.1 Uniform light intensity

To obtain uniform light intensity on the resin surface, where non-uniform intensity causes uneven photopolymerization and distortion of the final microstructure, μ SL was manually aligned and the intensity profile was measured using a large area imager (LBA-USB-L11058, Ophir-Spiricon Inc., Logan, UT). Two cross-sections of the design of sleeve were used to generate patterns on the imager.

3.3.2 Viscosity control

Generally, μ SL requires the use of a low viscosity photocurable resin, because it uses a deep-dip process to refresh the resin surface (Varadan et al., 2001; Choi et al., 2009a). The main material, DSM Somos[®] ProtoTherm[™] 12120 as a commercial resin, has \sim 410 cP as a nominal viscosity at 30

°C, which is relatively high to be used in μ SL. To reduce the viscosity, ProtoThermTM was blended with PNGD as a diluent, and the viscosity was measured using a Brookfield viscometer (DV-E, Middleboro, MA) according to the mixture ratio such as 100: 0, 90: 10, 80: 20, 70: 30, 60: 40, and 50: 50 (ProtoThermTM: PNGD) at room temperature (24 °C). In μ SL, viscosity values small than 200 cP is recommended for fast recoating with thin layer thickness (Varadan et al., 2001; Choi et al., 2009a, 2009b)

3.3.3 Cure depth control

In general, a commercial resin is compatible with macro-scale structures, and it has relatively large penetration depth of the light (D_p), e.g., 0.14 mm and low critical exposure energy (E_c), e.g., 12.2 mJ/cm² for ProtoThermTM. Large D_p leads overcure and occlusion in overhanging micro-features, thus cure depth needs to be controlled (Choi et al., 2009a). In addition to the large D_p , the main material was diluted, thus there exists no information about curing characteristics (D_p and E_c), which would be used for determining process parameters such as exposure energy and others. First,, to control cure depth, Tinuvin 400 as a light absorber at a concentration of 1.0 wt% was used, and in order to determine the specific curing characteristics of the mixture a curing experiment was conducted. D_p and E_c can be calculated from the Beer-Lambert formula provided in Eq. (1) (Jacobs, 1993). Cure depth (C_d) was measured using a crossbeam, which was produced by varying exposure energy (E_{max}) at the resin surface (Zissi et al., 1996; Choi et al., 2009a, 2009b). The exposure energy was controlled by adjusting exposure time of the lamp such as 10 s, 12 s, 14 s, 16 s, 18 s, 20 s, and 22 s. Eight crossbeams were built for each exposure time.

$$C_d = D_p \ln (E_{max}/E_c) \quad (1)$$

3.3.4 Multiple exposure for segmented region

Even though cure depth can be controlled using a light absorber, a desired microstructure having overhanging micro-features with different slopes may not be obtained (Choi et al., 2009a). This is because an overhanging feature having a gentle slope is more affected by the penetration depth than a feature having a steep slope. Contrarily certain amount of overcure is important to ensure that the currently cured layer is attached to the previously built layer, and weak exposure energy often leads to distortion of microstructures after building. Thus, both of cure depth control and overcure play an important role in producing microstructures. However, both of them cannot be satisfied at the same time because cure depth control directly affects an amount of overcure.. This contradiction may be partially solved by process planning according to a geometry (Limaye and Rosen, 2006, 2007) and multiple exposures for segmented regions (Park et al., 2009). In this paper, the micro-vane and hollow tube features as shown in Fig. 3 were separately cured using multiple exposures with different energy. This was accomplished by saving and slicing separate solid models for the micro-vane and hollow tube and using different exposure times for each model. That is, a relatively long exposure time was used

for the hollow tube to ensure that it can stand alone and any distortion does not occur after build, whereas a short exposure time was used for obtaining fine features of the micro-vane, which does not prevent the flow of solution. By comparing micro-vanes fabricated with and without multiple exposures for segmented regions, the introduced method was verified. Sleeves with the micro-vane were fabricated using the process parameters as described in Table 1. The rectangular section of micro-vane with the size of 0.219 mm × 0.110 mm was measured using a stereomicroscopic (Leica MZ16, Leica Microsystems, Switzerland) to confirm the feasibility of the use of the multiple exposure.

Table 1 Process parameters for producing a sleeve in μ SL

Total layer number		832
Layer thickness (μ m)		18
Settling time (sec)		10
Irradiance (mW/cm^2)		26.4
Single exposure time (sec)		15 ~ 20
Multiple exposure time (sec)	Sleeve	25
	Vane	15 ~ 20
Total fabrication time (hour)		7 ~ 10

3.3.5 Flow velocimetry

Using the fabricated sleeve with the micro-vane, flow velocimetry was measured through PIV. Tracer particles (S-HGS Silver-coated hollow glass sphere, Dantec dynamics) were mixed in the irrigation fluid and water container, and pulsed laser light sheet, which was produced by Nd-YAG laser (30 mJ/pulse, 15 Hz, Solo PIV, New Wave Research Inc), illuminated the particles. The laser light sheet was radiated twice within a short interval of time, and a CCD camera (TM-1325CL, JAI/Pulnix Inc) captured these scattering light images on two successive frames. By using these images, the displacement of the tracer particles in the image was analyzed by cross-correlation function. To evaluate the physical position and displacement of tracer particles in the image, a calibration plate, which has grid holes with 0.5 mm intervals, was inserted into the measurement plane in a fluid imaged by the CCD cameras. Based on this image, the pixel position named ‘Image coordinate’ was associated with the physical position by the second order polynomial warping function. The velocity of the tracer particles was obtained by dividing the displacement of the tracer particles by interval time of the radiated laser light sheets.

4. Results and Discussion

4.1 Uniform light intensity

The measured intensity profiles as shown in Fig. 5 show that the focused pattern on the resin surface has a uniform intensity, thus it can be thought that the system was properly aligned for achieving microstructures. In particular, because the designed sleeve has both the thin wall and fine micro-vane, a non-uniform intensity on the resin surface cause a distortion of the final sleeve. Additionally,

bending of the sleeve might occur because the sleeve is a relative high-aspect ratio (~ 7.4) microstructure. However, it is noted that distortion and bending of the sleeve may also be affected by exposure energy and other process parameters. Thus, it could be expected that the aligned system with the uniform intensity would take a share of producing a straight sleeve without distortion.

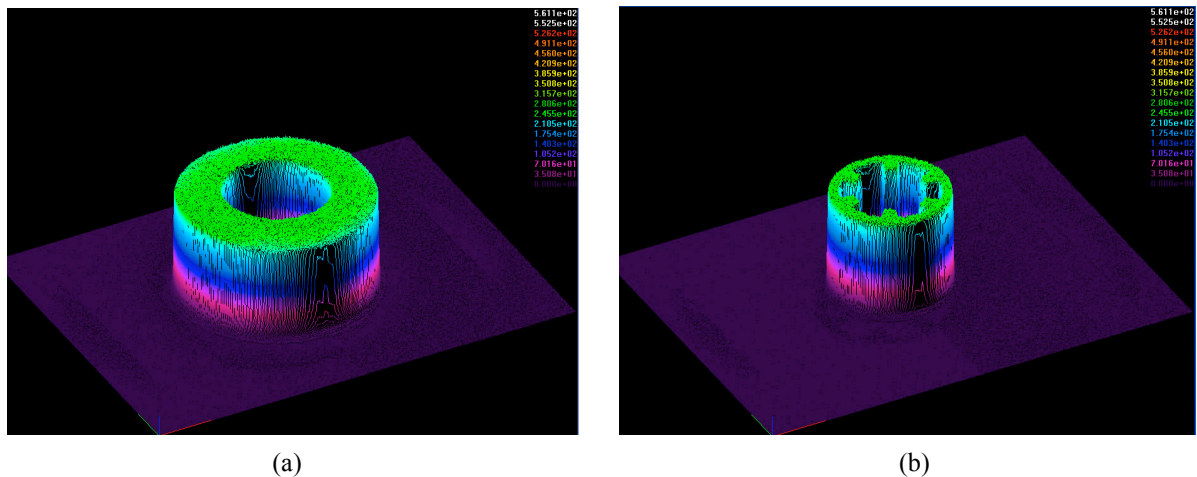


Fig. 5 Light intensity profile: (a) bottom section. (b) top section with vane (Note that the color bars in the figures represent not absolute values, but relative values. The average intensity of the green part was $\sim 26.35 \text{ mJ/cm}^2$).

4.2 Viscosity control

Fig. 6 shows the measured viscosity of the ProtoThermTM 12120 diluted with PNGD. The graph shows that the viscosity exponentially decreased as the amount of PNGD increased. The initially measured viscosity without the diluents at room temperature was $\sim 1100 \text{ cP}$, which is relatively higher than the viscosity ($\sim 410 \text{ cP}$) provided from the company, and it is thought that the viscosity increased as time elapsed. The viscosity for a 50:50 mixture (ProtoThermTM: PNGD wt%) was measured to be $\sim 100 \text{ cP}$, and this mixture was chosen for producing the sleeve.

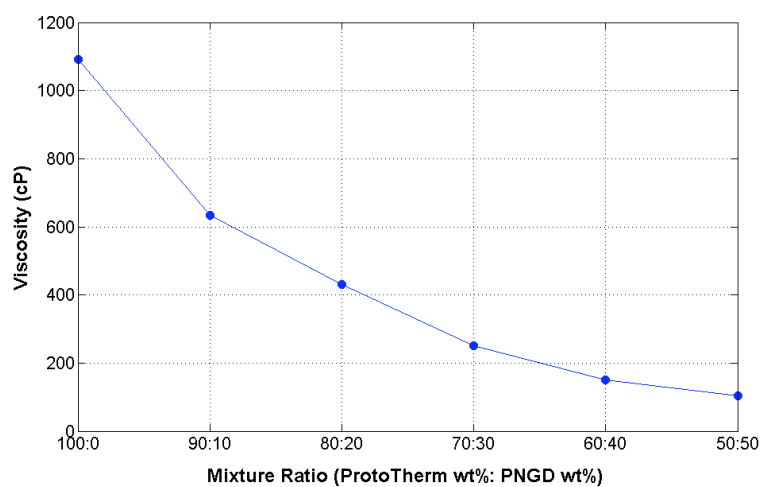


Fig. 6 Viscosity variation according to the mixture ratio

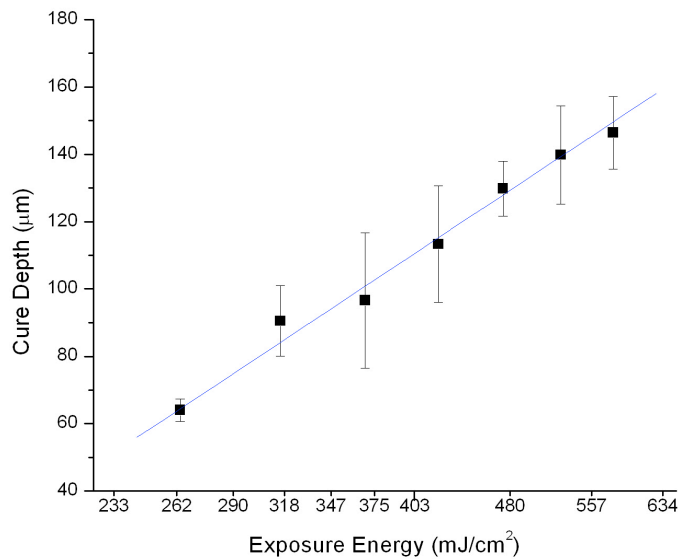


Fig. 7 Measured cure depth by varying exposure energy (A natural log scale was used for X axis and the error bars represent plus/minus one standard deviation).

4.3 Cure depth control

Cure depth was controlled by blending Tinuvin 400 as a light absorber, and Fig. 7 represents measured cure depths according to energy dosage on the resin surface. By regressing the measured data, D_p and E_c were determined $\sim 108 \mu\text{m}$ and 145 mJ/cm^2 . Compared to the curing characteristics about ProtoThermTM as a main material, D_p was decreased $\sim 22.9 \%$ and E_c was increased $\sim 1089 \%$. Even though the calculated D_p is small than the original value ($\sim 140 \mu\text{m}$) of ProtoThermTM, it is relatively larger than that used by other researches (Choi et al., 2009a, 2009b). However it was expected that a minimum achievable feature size would be about $\sim 100 \mu\text{m}$, and it is a relevant value for producing micro-vane.

4.4 Multiple exposure

The thickness and width of micro-vane according to the exposure time were measured and Fig. 8 shows the results for multiple and single exposure. The measured micro-vane thickness using multiple exposure was 40 % \sim 81 % larger than the designed dimension ($110 \mu\text{m}$), whereas the thickness using single exposure was 121 % \sim 319 % increased. Additionally, micro-vane widths using multiple and single exposure were 38 % \sim 40 % and 21 % \sim 45 %, respectively, smaller than the designed width ($219 \mu\text{m}$). Using multiple exposure it was possible to obtain thinner micro-vane, it was, however, detached or broken from the sleeve. Even though the exact dimensions were not achieved, multiple exposure fabrication has better result of obtaining thinner micro-vane. Fig. 9 shows the fabricated micro-vane inside the sleeve with and without multiple exposure when the exposure time was 15 s.

According to Fig. 9 it might occur that the overcured micro-vane by single exposure occludes the path of solution flow. Additionally, relatively short exposure time often resulted in distortion in the sleeve as shown in Fig. 10 when rinsing and post-curing. Thus it can be thought that multiple exposure is effective mean to obtain fine feature of the micro-vane. Finally it is recommended that exposure times for sleeve and micro-vane have to be more than 20 s and 15 s ~ 20 s, respectively. Fig. 11 shows the fabricated sleeve using exposure time of 30 s and 20 s for the hollow tube and micro-vane.

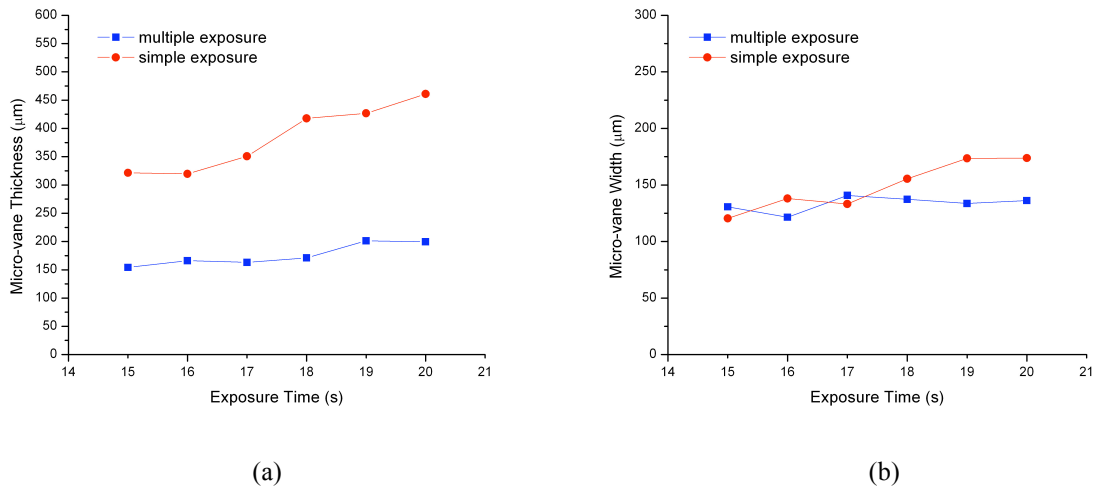


Fig. 8 Measured micro-vane dimensions with and without multiple exposure: (a) micro-vane thickness, (b) micro-vane width

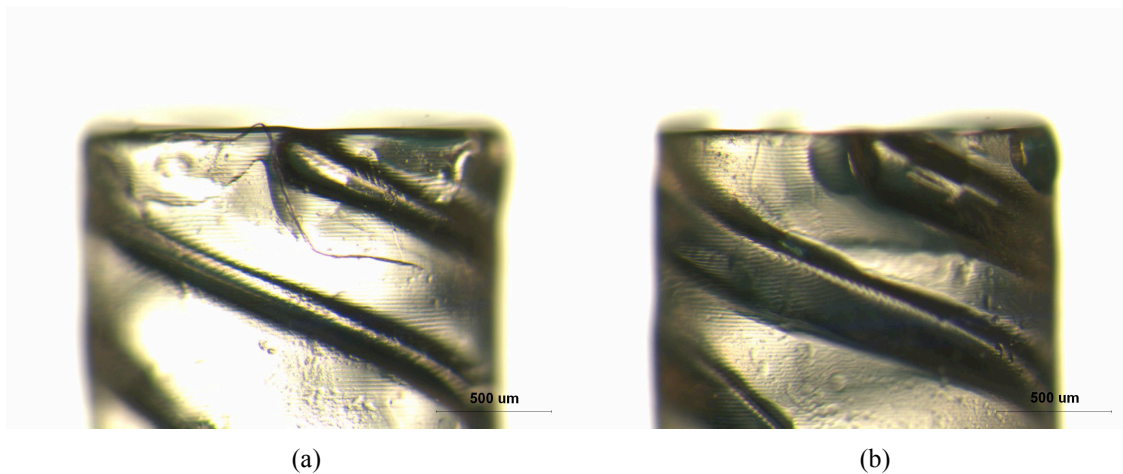


Fig. 9 Optical micrographs of micro-vanes fabricated using 15 s exposure time: (a) with and (b) without multiple fabrication.

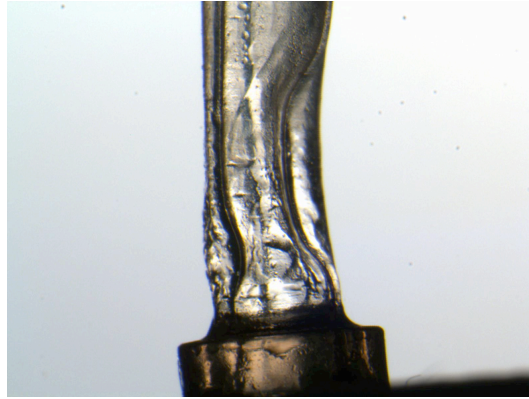


Fig. 10 Optical micrographs of distorted sleeve



Fig. 11 Successfully built sleeve using multiple exposure

4.5 Integration

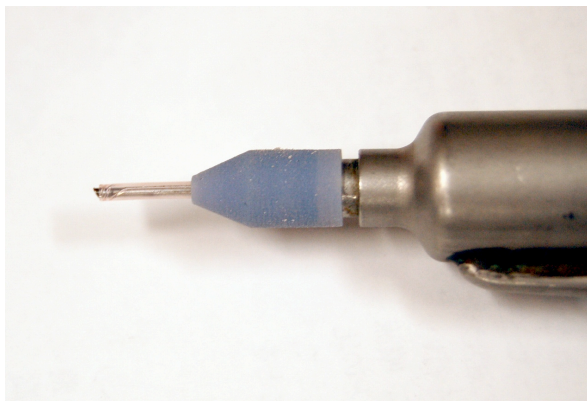
The sleeve with micro-vane fabricated with the μ SL system and the threaded fitting fabricated with the Eden 333 system were integrated as shown in Fig. 12. Both of sleeve and threaded fitting were successfully built for integration and Fig. 13 shows a phacoemulsifier with the fabricated sleeve and threaded fitting.



Fig. 12 Integrated sleeve and threaded fitting.



(a)



(b)

Fig. 13 Phacoemulsifier equipped with 3D micro-vane within the sleeve: (a) phacoemulsifier with the fabricated sleeve, (b) magnified image of the sleeve

4.6 Flow velocimetry

We measured the velocity distribution with 0.5mm intervals when the tip was submerged in the water container. Measurement plane is normal to the axis of the tip. Fig 14 shows mean velocity vectors. The position of the measurement planes located at 1.0mm, 1.5mm, 2.0mm, 2.5mm and 3.0mm from the head of the tip. Color indicates magnitude of velocity. It can be confirmed that water was irrigated from the head of tip, and irrigation gushed in three radial directions.

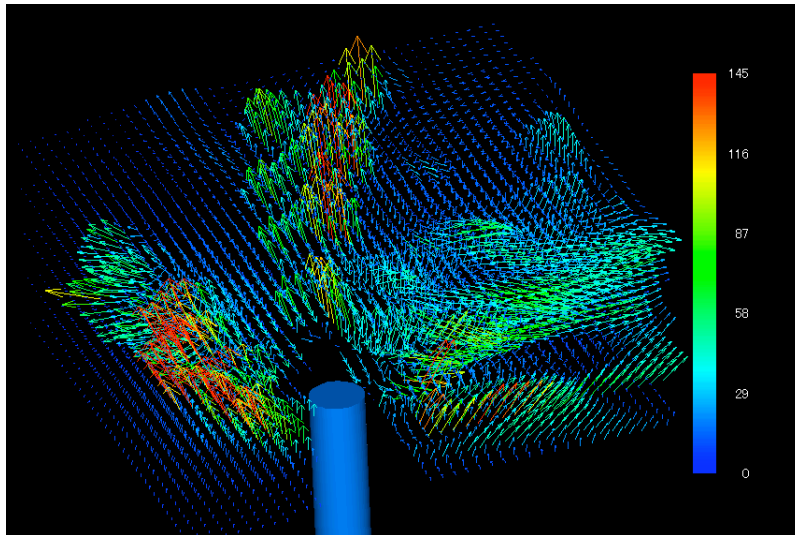


Fig. 14 Flow velocimetry.

5. Conclusions

In this work, the successful fabrication in use of sleeve with a 3D micro-vane, which is used in phacoemulsification for cataract surgery, was demonstrated. The 3D micro-vane was suggested for introducing swirl into the irrigation solution and dissipating flow velocities from the irrigation solution on the corneal endothelial cells in the inner eye. To fabricate 3D micro-vane within a sleeve, a two-part design for a threaded fitting, which can be assembled with a phacoemulsifier, and sleeve with micro-vane, which can be integrated with the threaded fitting. Both of designed parts were fabricated using a commercial additive manufacturing system and microstereolithography system. Compared to fabrication in commercial additive manufacturing system, microfabrication required reforming of material properties and adjusting process parameters for producing micro-features. To accomplish microfabrication in microstereolithography, the fabrication system was manually aligned and verified by inspecting pattern intensity, and it was confirmed that the focused light had uniform light intensity. Cure depth of the material were controlled by blending a light absorber, and finally they were suitable for producing 3D micro-vane. Additionally, for obtaining a non distorted sleeve with 3D micro-vane, multiple exposure was conducted, and results show that the suggested multiple exposure is a promising mean for producing a final sleeve with 3D micro-vane. Finally the new combined device was tested in a water container using particle image velocimetry, and the results showed the irrigation fluids

ejecting through the micro-vane towards the three radial directions. In conclusion, it is believed that this new device will reduce damage to endothelial cells during cataract surgery and significantly improve patient outcomes from this procedure, and this unique application demonstrates the utility of combining μ SL with a macro rapid prototyping technology for fabricating a real macro-scale device with functional, 3D micro-scale features that could not be fabricated using conventional methods. In the future, the phacoemulsifier with the developed sleeve will be tested in cow eyeballs to show significant reductions in flow velocities and resulting shear stresses on the endothelial cells.

References

- A. Bertsch, S. Zissi, J.Y. Jézéquel, S. Corbel, and J.C. André, *Microsyst. Technol.* **3**, 42-47 (1997).
- A. Bertsch, S. Zissi, J.Y. Jézéquel, S. Corbel, and J.C. André, *Microstereolithography: concepts and applications*. Proc. 8th IEEE Int. Conf. Emerging Technologies and Factory Automation, 289-98 (2001).
- A. Bertsch, S. Jiguet, and P. Renaud, *J. Micromech. Microeng.* **14**, 197-203 (2004).
- A.M. Jousen, U. Barth, H. Çubuk, and H.R. Koch, *J. Cataract. Refract. Surg.* **26**, 392-397 (2000).
- A.S. Limaye, and D.W. Rosen, *Rapid Prototyping J.* **12**, 283-291 (2006).
- A.S. Limaye, and D.W. Rosen, *Rapid Prototyping J.* **13**, 76-84 (2007).
- C. Born, Z. Zhang, M. Al-Rubeai, and C.R. Thomas, *Biotechnol. Bioeng.* **40**, 1004-1010 (1992).
- C. Sun, and X. Zhang, *J. Appl. Phys.* **92**, 4796-4802 (2002).
- C. Sun, N. Fang, D.M. Wu, and X. Zhang, *Sens. Actuator A-Phys.* **121**, 113-120 (2005).
- D. Gajjar, M.R. Praveen, A.R. Vasavada, D. Pandita, V.A. Vasavada, D.B. Patel, K. Johar, and S. Raj, *J. Cataract. Refract. Surg.* **33**, 2129-2134 (2007).
- F.M. Polack, and A. Sugar, *Invest. Ophthalmol.* **15**, 458-469 (1976).
- I.B. Park, Y.M. Ha, and S.H. Lee, *Int. J. Adv. Manuf. Technol.* Published online: 07 May 2009, DOI 10.1007/s00170-009-2065-0
- J.W. Choi, Y.M. Ha, S.H. Lee, and K.H. Choi, *J. Mech. Sci. Technol.* **20**, 2094-2104 (2006).
- J.W. Choi, R.B. Wicker, S.H. Cho, C.S. Ha, and S.H. Lee, *Rapid Prototyping J.* **15**, 59-70 (2009).
- J.W. Choi, R. Wicker, S.H. Lee, K.H. Choi, C.S. Ha, and I. Chung, *J. Mater. Process. Technol.* Published online: 13 May 2009, DOI: 10.1016/j.jatprotec.2009.05.004
- K. Ikuta, and K. Kirowatari, *Real three dimensional micro fabrication using stereo lithography and metal molding*. Proc. Int. Conf. MEMS. 42-47 (1993).
- K. Hayashi, H. Hayashi, F. Nakao, and F. Hayashi *J. Cataract. Refract. Surg.* **22**, 1079-1084 (1996).
- K.M. Lee, H.G. Kwon, and C.K. Joo, *J. Cataract. Refract. Surg.* **35**, 874-880 (2009).
- L.H. Han, G. Mapili, S. Chen, and K. Roy, *J. Manuf. Sci. Eng.-Trans. ASME* **130**, 021005-1-4 (2008).
- M. Topaz, M. Motiei, and E. Assia, *Ultrasound Med. Biol.* **28**, 775-784 (2002).
- M.W. Miller, D.L. Miller, and A.A. Brayman, *Ultrasound Med. Biol.* **22**, 1131-1154 (1996).
- O. Thoumine, T. Znegler, P.R. Girard, and R.M. Nerem, *Exp. Cell Res.* **219**, 427-441 (1995).
- P.D. O'Brien, P. Fitzpatrick, and D.J. Kilmartin, S. Beatty, *J. Cataract. Refract. Surg.* **30**, 839-843

(2004).

- P.F. Jacobs, *Rapid Prototyping and Manufacturing: Fundamentals of Stereolithography*, McGraw-Hills, New York, NY (1993).
- P. Regenfuss, A. Streek, L. Hartwig, S. Klötzer, Th. Brabant, M. Horn, R. Ebert, and H. Exner, *Rapid Prototyping J.* **13**, 204-212 (2007).
- P.S. Binder, H. Sternberg, M.G. Wickham, and D.M. Worthen, *Am. J. Ophthalmol.* **82**, 48-54 (1976).
- R.F. Steinert, and M.E. Schafer, *J. Cataract. Refract. Surg.* **32**, 284-287 (2006).
- R.H. Osher, and V.P. Injev, *J. Cataract. Refract. Surg.* **33**, 401-407 (2007).
- S.J. Lee, H.W. Kang, T.Y. Kang, B. Kim, G. Lim, J.W. Rhie, and D.W. Cho, *J. Micromech. Microeng.* **17**, 147-153 (2007).
- S.J. Lee, H.W. Kang, J.K. Park, J.W. Rhie, S.K. Hahn, and D.W. Cho, *Biomed. Microdevices* **10**, 233-241 (2008).
- S. Khalil, and W. Sun, *Mater. Sci. Eng. C-Biomimetic Supramol. Syst.* **27**, 469-478 (2007).
- S. Zissi, A. Bertsch, J.Y. Jézéquel, S. Corbel, D.J. Lougnot, and J.C. André, *Microsyst. Technol.* **2**, 97-102 (1996).
- V.K. Varadan, X. Jiang, and V.V. Varadan, *Microstereolithography and Other Fabrication Techniques for 3D MEMS*, (Wiley, West Sussex, 2001).
- Y. Kaji, T. Oshika, T. Usui, and J. Sakakibara, *Cornea* **24**, S55-S58 (2005).
- Y.M. Ha, J.W. Choi, and S.H. Lee, *J. Mech. Sci. Technol.* **22**, 514-521 (2008).